Egyptian Knowledge Bank
https://ijmti.journals.ekb.eg/

International Journal of Materials Technology and Innovation
Volume 4, Issue 2 (2024), pages 39-45

Online ISSN 2682-4299

Effect of Wire Arc Additive Manufacturing Process Parameters on Bead Geometry and Porosity Formation of 5356 Aluminum alloy

Eman Shams[1, 3*], M. Abdelwahed[1], Noha Ramadan[1], Mohammed Ibrahim Awad[2], Nahed El-Mahallawy[1], Mohamed A. Taha[1]

[1]Design and Production Engineering Department, Faculty of Engineering, Ain-Shams University, 11517 Cairo, Egypt
[2]Mechatronics Engineering Department, Faculty of Engineering, Ain-Shams University, 11517 Cairo, Egypt
[3]Mechanical Engineering Department, Faculty of Engineering, Nahda University, New Bani Sweif, Egypt

*Corresponding author: E-mail: eman.shams@nub.edu.eg

Received ….... 24 Nov. 2024
Accepted …….26 Dec. 2024
Published .....31 Dec. 2024

Abstract

Wire Arc Additive Manufacturing holds significant promise for producing large, intricate aluminum parts with reduced cost and material waste. This study aims to investigate the influence of process parameters on the porosity formation and bead geometry of aluminum alloy ER5356, including voltage, scanning speed, and energy density. A series of 36 single-track aluminum samples were fabricated under varying welding conditions. The results show that increasing voltage enhances bead width and penetration but reduces height and contact angle. Similarly, higher scanning speeds result in smaller bead dimensions. Energy density influenced both bead geometry and porosity, with higher energy densities increasing porosity. The investigation revealed that the most effective voltage range for achieving consistent track formation is between 22 and 24 V. In addition, it was found that higher scanning speeds and lower energy densities reduced porosity. These insights are crucial for refining Wire Arc Additive Manufacturing parameters for aluminum alloys, decreasing defects, and improving material performance for industrial uses.

Keywords: Wire Arc Additive Manufacturing, Gas Metal Arc Welding, ER5356 Aluminum Alloy, porosity, bead geometry.

1. Introduction

Additive manufacturing is a 3D printing technology which creates 3D shapes by depositing various materials using 3D-designed digital geometry information that is input into a manipulator [1–5]. Metal additive manufacturing methods have generated attention because of their superiority over traditional manufacturing methods in creating intricate and nearly perfectly shaped components with minimal material waste [1]. The direct energy deposition method is regarded as one of the principal techniques in metal additive manufacturing, which can be categorized into powder-based and wire-based [2], as illustrated in Figure 1.

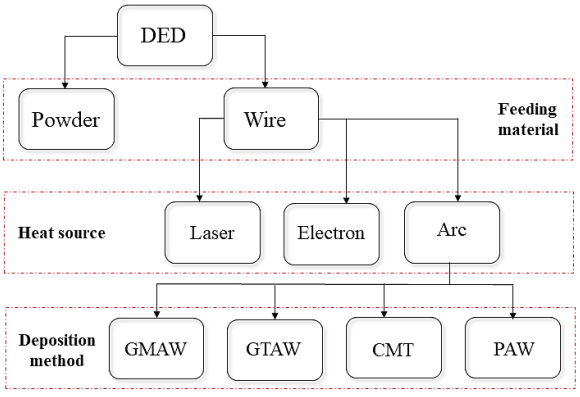

Fig. 1 Summarization of direct energy deposition [1]

IJMTI vol. 4 issue 2 (2024) 39-45 https://doi.org/10.21608/ijmti.2024.338250.1117

Wire arc additive manufacturing is a method which uses wire as feedstock. The material is then deposited using an electric arc between the substrate and wire [3], as schematically presented in Figure 2.

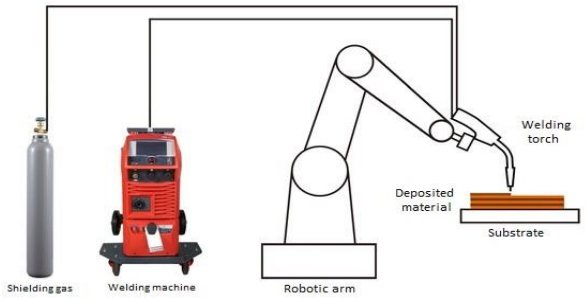

Fig. 2 Wire arc additive manufacturing methodology [2]

In addition, wire feedstocks are cheaper, more widely available, and safer to manage than metal powder feedstocks for Additive Manufacturing processes, potentially impacting the final product cost [4]. Various heat sources, including Gas Metal Arc Welding [3], Gas Tungsten Arc Welding [5], Cold Metal Transfer [6], and plasma Arc Welding [7], can be integrated into wire arc additive manufacturing systems. The heat source selection depends on the requirements for the final product quality and the chosen material. One of the key benefits of wire arc additive manufacturing is its ability to produce large parts with intricate geometries [8], potentially reducing process cost and time comparing to other traditional methods [9-11]. In gas metal arc welding processes, spattering results from excess energy density. As a result, it is necessary to manage the high energy densities to weld metals (such as aluminium) with lower melting points.

Wire arc additive manufacturing has diverse applications in the automotive, aerospace, and medical industries, where metal components with complex geometries and high mechanical properties are needed [12, 13].

S. K. Manjhi et al. [14] analysed the impact of wire feeding speed and scanning speed on the width, penetration, height, and contact angle of the bead of nine deposited single tracks. They found that raising the wire feeding speed increased the voltage and current, which in turn resulting in higher energy density in melt pool. This caused dynamic forces in the weld pool, a rise in temperature, and decreased viscosity of melted metal. As a result, the melted metal droplet spread across the substrate, increasing width, contact angle, and penetration.

Another research by S. Li et al. [15] concluded that bead width, contact angle, and height decreased as the scanning speed increased. As the current grew, so did the bead width, penetration, and height, but there is no significant effect on contact angle. As the voltage increased, the bead width, penetration, and height did not vary considerably, but contact angle dropped simultaneously.

Köhler et al. [16] employed wire arc additive manufacturing to fabricate aluminium wires and monitored the change in bead geometry based on the interlayer temperature. An increase in wire feed speed and scanning speed resulted in a decrease in layer height. A higher interlayer temperature also led to the aluminium fabricated part's larger width and height.

Fang et al. [17] compared the mechanical properties of aluminium components based on the arc mode of a cold metal transfer welding machine. The study revealed variations in mechanical properties due to changes in the arc mode at the same current and voltage conditions.

Based on literature, few research conducted filler wire 5356 to deposit it on 7XXX series substrate, and non-research used 7108 aluminium substrate, due to their low thermal conductivity. So, it was a challenge to use these two different alloy series to fabricate these single tracks using MIG arc mode.

This study involves the trials to manufacture aluminium components via wire arc additive manufacturing and analyses the variations in the bead geometry of the single tracks based on different welding parameters. The impact of energy density, voltage, and scanning speed on the bead geometry and pores formation was assessed across 36 welding conditions to find optimized process parameters.

2. Experimental Work

2.1. Materials

The filler wire material is aluminium alloy ER5356 with a 1.2 mm diameter, while the substrate material used is 100×46×20 mm3 aluminium 7108. The chemical composition of filler wire and substrate materials is presented in Table 1. The substrate was prepared by grinding using the turning machine to achieve a flat surface. Then, it was cleaned with acetone immediately before deposition to remove oil stains and oxide films.

IJMTI vol. 4 issue 2 (2024) 39-45 https://doi.org/10.21608/ijmti.2024.338250.1117

Table 1 The chemical compositions of the used filler wire and substrate (wt.%)

No.	Chemical Composition, %					
	Mg	Zn	Mn	Ti	Fe	Al
Filler wire	5.59	0.003	0.16	0.09	0.27	Bal.
Substrate	0.77	4.95	0.03	0.02	0.15	Bal.

2.2 Wire arc additive manufacturing procedures

The experiments were performed using Jess 325 MIG heat source combined with a four-axis robotic system which is 3 linear axes (X, Y, Z) and rotating axis, as shown in Figure 3. The welding torch is fixed at Z-axis, which is used for the movement, which manipulated using a control system, that helped to convert the G code for the fabrication process into a digital signal for the robotic system. The welding torch moved upwards along the Z axis by a constant distance for each single track. 99.999% pure Argon gas was used to maintain an inert environment during deposition. The substrate upon is fixed at the base block. The welding torch was held vertically, and the aluminium filler wire entered through the welding torch to deposit the bead.

Fig. 3 Schematic view of gas metal arc welding-based system

The processing parameters were selected to systematically study their influence on bead geometry and porosity formation in the WAAM process. Voltage and scanning speed ranges were chosen to cover a wide range of energy densities. Fixed parameters, used to ensure consistent welding conditions. This experimental design provided comprehensive insights into the relationship between energy input and weld quality, enabling identification of optimal settings for defect reduction and enhanced fusion. Process parameters are set as constant: the wire feeding speed at 7.5 m/min, 7 mm standoff distance, 50 mm single track length, 18 L/min flow rate of the shielding gas, and the welding efficiency is set to 0.8. Eight values of scanning speed have been tested in this study in a range from 250 to 500 mm/min, and thirteen voltage values have been tested in a range from 15 to 29 V. The parameters used to fabricate 36 single-track samples are presented in Table 2. The energy density (E) was calculated using equation (1).

$$E = \frac{v * I * \eta * 60}{Sc} \qquad eq.1$$

E is the energy density in J/mm, V is the voltage in Volt, I is the current in Amperage, η is the welding efficiency, and Sc is the scanning speed in mm/min.

Table 2 Processing parameters of single welded beads

Track No.	Printing machine parameters	Welding machine parameters		
	Sc (mm/min)	I (Amperage)	V (Volt)	E (J/mm)
1	350	116.80	15	240.27
2	350	100.29	17	233.82
3	350	112.00	20	307.20
4	250	93.34	21	376.35
5	300	98.54	21	331.09
6	350	101.32	21	291.80
7	350	114.40	21	329.47
8	400	103.24	21	260.16
9	450	96.94	21	217.15
10	500	94.20	21	189.91
11	350	114.90	22	346.67
12	250	126.09	23	556.81
13	250	124.36	23	549.17
14	300	105.92	23	389.79
15	300	120.45	23	443.26
16	350	122.61	23	386.75
17	350	125.89	23	397.09
18	350	120.35	23	379.62
19	400	114.50	23	316.02
20	450	123.94	23	304.07
21	500	119.43	23	263.70
22	250	116.04	24	534.71
23	250	121.48	24	559.78
24	300	117.86	24	452.58
25	300	120.20	24	461.57
26	350	122.61	24	403.56
27	350	126.28	24	415.64
28	350	115.09	24	378.81
29	400	114.83	24	330.71
30	450	117.75	24	301.44
31	500	114.29	24	263.32
32	350	122.19	25	418.94
33	350	131.50	26	468.89
34	350	118.85	27	440.08
35	350	130.27	28	500.24
36	350	179.75	29	714.89

IJMTI vol. 4 issue 2 (2024) 39-45 https://doi.org/10.21608/ijmti.2024.338250.1117

2.3. Bead Characterization

2.3.1. Track appearance and characterization

All single tracks have been visually inspected, and the geometry of the welded beads has been analysed; the bead width has been measured using a stereo microscope. The geometry for the welded bead is defined by W = Bead width, P = Penetration, H = Bead height, and θ = Contact angle, as shown in Figure 4. Inventor software is used to measure the characteristics of the bead, including the welded bead width, penetration (fusion zone), height, and contact angle.

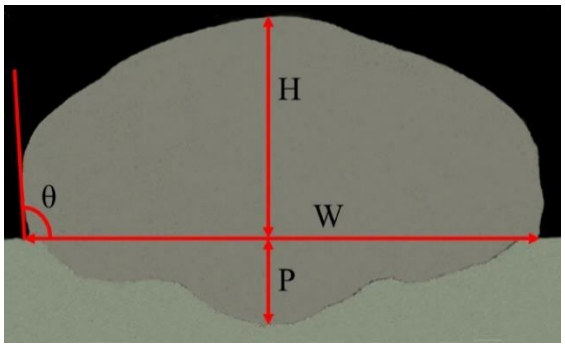

Fig. 4 Definition of the bead geometry, W = Bead width, P = Penetration, H = Bead height, and θ = Contact angle

2.3.2. Microscopic investigation

The samples for microstructure analysis were cut using a wire cutting machine, mounted in cold epoxy resin, and ground with 220, 320, 400, 600, 800, 1000, 1200, 2000, 2500, and 4000 grit sandpapers with flowing water coolant that was used to prevent any increase in material temperature during the process, which might affect the microstructure and mechanical properties. Finally, the samples were polished into a mirror finished using 0.5µ alumina powder (suspension solution), then washed using deionized water then ethanol, and dried with a dryer to get a clear image to calculate the percent of porosity, which was measured and calculated using Image J software.

3. Results and discussion

3.1. Track appearance and characterization

Voltages in the range of 15-21 V result in intermittent single tracks, which can be attributed to inconsistent welding—a typical surface morphology observed in the process due to low energy density, as seen in figure 5. In contrast, voltages between 22 and 24 V yield more consistent tracks owing to higher energy density, as illustrated in Figure 6.

Fig. 5 Intermittent single tracks using voltage in the range from 15 to 21 V

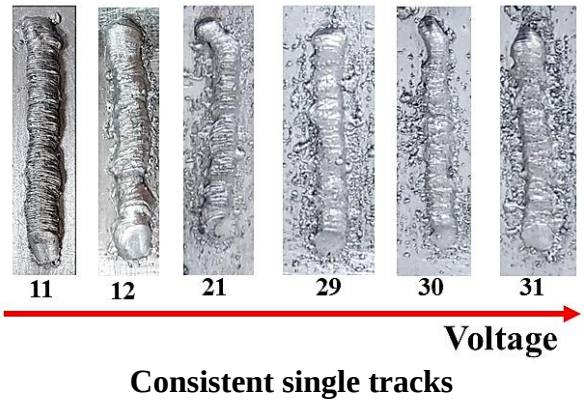

Fig. 6 Consistent single tracks using voltage in the range from 22 to 24 V

Higher voltages, specifically in the 23-29 V range, are associated with an increased likelihood of spatter formation, as depicted in Figure 7.

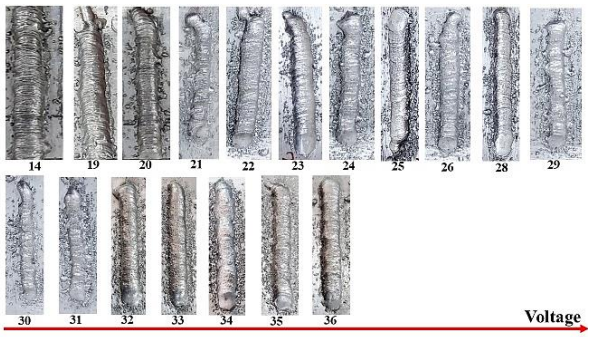

Fig. 7 Spatters in single tracks using voltage in the range from 23 to 29 V

A voltage of 21 V combined with scanning speeds of 250 and 300 mm/min produces the widest intermittent single tracks, as demonstrated in samples

IJMTI vol. 4 issue 2 (2024) 39-45 https://doi.org/10.21608/ijmti.2024.338250.1117

4 and 5. Conversely, a voltage of 24 V with scanning speeds ranging from 400 to 500 mm/min does not facilitate effective deposition, as observed in samples 29, 30, and 31.

A scanning speed of 350 mm/min is the most suitable for the fabrication process; however, as shown in samples 34, 35, and 36, attention must be paid to potential spatter formation at higher voltage levels.

Tracks 7, 13, 15, 16, 17, 18, 20, and 27 exhibit the best surface appearance and have been selected for further analysis, as shown in Figure 8.

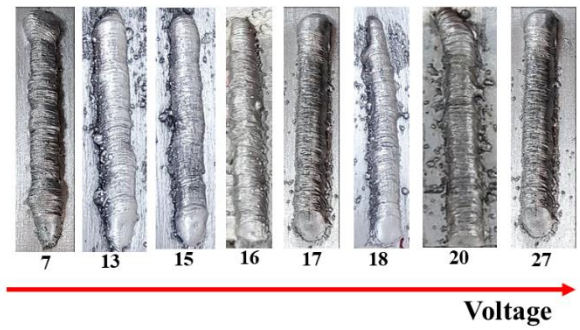

Fig. 8 Best appearance single tracks for further analysis

More than visually examining the best track morphology is required to understand and fully determine the best process parameters for deposition. Therefore, analyzing the width, penetration (fusion zone), height, and contact angle of these tracks' deposited beads is essential to identify appropriate process parameters.

3.2. Analysis of welded beads

The cross-sections of all welded beads for each single track have been examined. It has been observed that fusion zones may occur either partially or completely, regardless of the track's appearance—whether intermittent, spattered, or continuous. Partial fusion zones are typically found within an energy density range of 330-550 J/mm, that's because higher energy densities resulting in excessive heat input that may cause rapid melting, leading to a more turbulent molten pool which can disrupt uniform fusion with the substrate, resulting in areas of incomplete fusion (partial fusion zones). Complete fusion occurs within a lower energy density range of 304-329 J/mm, that's because lower energy density allows slower cooling and providing adequate time for material fusion across the substrate leading to complete fusion. Figure 9 illustrates the welded beads of the eight best-performing single tracks across various energy densities. Partial fusion zones appear in the middle of track 13, whereas complete fusion zones are present in tracks 7 and 20. The remaining single tracks exhibit a lack of fusion.

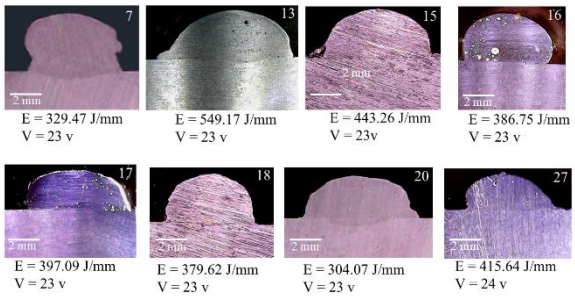

Fig. 9 Bead geometry of best eight single track samples

Table 3 records the calculated average percent of porosity and the measured geometry for the welded bead, defined by W = Bead width, H = Bead height, P = Penetration, and θ = contact angle. Figure 10 represents the cross-section photomicrograph for the whole section without etching, showing the porosity location for completely fused samples.

Table 3 Bead geometry for the best appearance single track samples

Track No.	W (mm)	H (mm)	P (mm)	Θ (°)	Average percent of porosity (%)
7	7.12	4.42	0.70	103	3.80
13	4.80	2.67	0.14	117	4.03
15	4.95	2.47	No	111	2.01
16	7.20	3.36	No	73	1.10
17	7.29	4.09	No	91	8.72
18	2.01	2.28	No	114	0.82
20	6.90	4.06	0.45	61	1.80
27	6.88	3.16	No	102	3.13

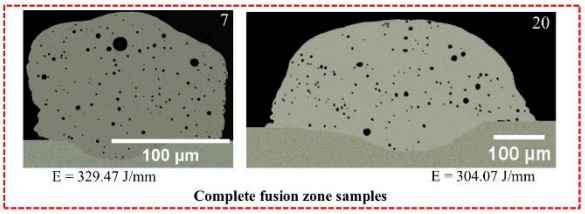

Fig. 10 Cross-section Photomicrograph for the completely fused single track samples.

Figures 11 and 12 illustrate the correlation between energy density and the width and height of the welded beads in this study and findings from the literature [14, 15]. As energy density increases, the dimensions of the beads are affected by the interaction between

IJMTI vol. 4 issue 2 (2024) 39-45 https://doi.org/10.21608/ijmti.2024.338250.1117

the 5356-aluminum wire and various substrates (7108, 7075, 5083). The variations in bead width can be primarily attributed to differences in thermal conductivity and alloy composition.

In case of the 5356-wire deposited on the 7075 substrates, the increase in bead width with rising energy density is linked to the lower thermal conductivity of 7075 relative to 7108. This property allows 7075 to retain heat more effectively, resulting in a larger molten pool and a wider bead as more material melts and spreads before solidifying. Conversely, when the 5356 wire is deposited on the 7108 substrates, the bead width initially shows a slight increase with rising energy density; however, beyond an energy density threshold of 400 J/mm, the rapid heat dissipation leads to quicker solidification, thereby reducing the molten pool size and, consequently, the bead width, despite the ongoing energy input. In instances where the 5356 wire is deposited on the same aluminum alloy series, the bead width increases with energy density. This is due to the uniform thermal conductivity of the wire and substrate, resulting in more even heat distribution and less heat dissipation than the 7108 substrates. Consequently, this facilitates greater melting of the material, leading to a wider molten pool and, thus, a wider bead.

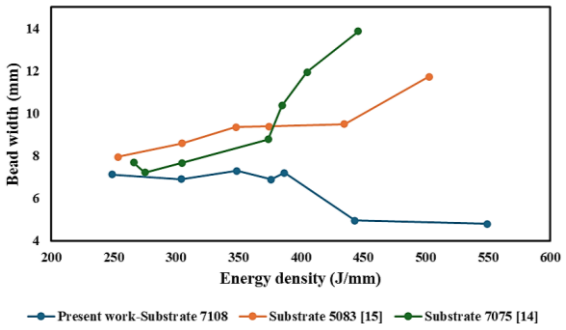

Fig. 11 Effect of energy density on the bead width

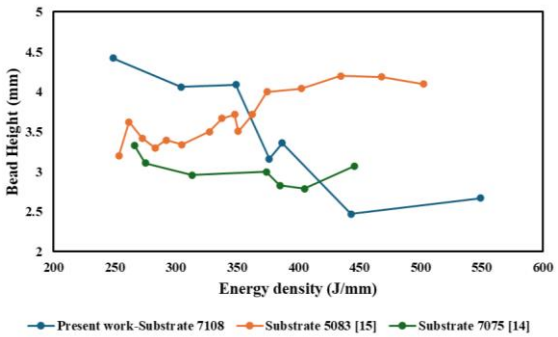

Fig. 12 Effect of energy density on the bead height.

4. Conclusions

The ability to fabricate intricate shapes with little material waste makes metal additive manufacturing technique better than other conventional techniques. The following are the study's main findings:

1. The study emphasizes how energy density and scanning speed greatly impact bead geometry, such as width, height, Penetration, and contact angle. A faster scanning rate yields a lower temperature and energy density, which reduces the width and height of the welded beads and promotes the creation of porosity.
2. Optimal voltage levels (22-24 V) contribute to consistent track formation, while excessive voltage can lead to spatter. Scanning speeds around 350 mm/min are identified as ideal for effective deposition.
3. This study shows that partial fusion is seen at greater energy density ranges (330-550 J/mm), whereas complete fusion zones are found within particular ranges (304-329 J/mm). This emphasizes the importance of energy input management to achieve the required weld quality.
4. Bead dimensions are influenced by the way aluminum wire interacts with different surfaces. For example, wider beads are produced by surfaces with lower thermal conductivity because they retain heat better. In order to maximize results, the study highlights the necessity of customized process settings based on material properties.

References

1. W. Zhai, N. Wu, and W. Zhou, “Effect of Interpass Temperature on Wire Arc Additive Manufacturing Using High-Strength Metal-Cored Wire,” Metals (Basel)., vol. 12, no. 2, 2022, doi: 10.3390/met12020212.
2. L. Zhang, S. Wang, H. Wang, J. Wang, T. Wang, and X. Dai, “Investigate the effect of arc characteristic on the mechanical properties of 5A56 Al alloy in CMT arc additive manufacturing,” CIRP J. Manuf. Sci. Technol., vol. 40, pp. 102–113, 2023, doi: 10.1016/j.cirpj.2022.10.006.
3. E. Eimer, S. Williams, J. Ding, S. Ganguly, and B. Chehab, “Mechanical performances of the interface between the substrate and deposited material in aluminium wire Direct Energy Deposition,” Mater. Des., vol. 225, p. 111594, 2023, doi: 10.1016/j.matdes.2023.111594.
4. C. R. Cunningham, J. M. Flynn, A. Shokrani, V. Dhokia, and S. T. Newman, “Invited review

article: Strategies and processes for high quality wire arc additive manufacturing," Addit. Manuf., vol. 22, pp. 672–686, 2018, doi: 10.1016/j.addma.2018.06.020.
5. D. Curiel, F. Veiga, A. Suarez, and P. Villanueva, "Advances in Robotic Welding for Metallic Materials: Application of Inspection, Modeling, Monitoring and Automation Techniques," Metals, vol. 13, no. 4. MDPI, Apr. 01, 2023. doi: 10.3390/met13040711.
6. T. S. Senthil, S. R. Babu, M. Puviyarasan, and V. S. Balachandar, "Experimental investigations on the multi-layered SS316L wall fabricated by CMT-based WAAM_ Mechanical and microstructural studies," J. Alloy. Metall. Syst., vol. 2, no. May, p. 100013, 2023, doi: 10.1016/j.jalmes.2023.100013.
7. C. S. Wu, L. Wang, W. J. Ren, and X. Y. Zhang, "Plasma arc welding: Process, sensing, control and modeling," J. Manuf. Process., vol. 16, no. 1, pp. 74–85, 2014, doi: 10.1016/j.jmapro.2013.06.004.
8. C. Xia et al., "A review on wire arc additive manufacturing: Monitoring, control and a framework of automated system," J. Manuf. Syst., vol. 57, no. August, pp. 31–45, 2020, doi: 10.1016/j.jmsy.2020.08.008.
9. N. Izan et al., "Process and Heat Resources for Wire Arc Additive Manufacturing of Aluminium Alloy ER4043 : A Review," vol. 20, no. 1, pp. 21–41, 2023.
10. K. Oyama, S. Diplas, M. M'hamdi, A. E. Gunnæs, and A. S. Azar, "Heat source management in wire-arc additive manufacturing process for Al-Mg and Al-Si alloys," Addit. Manuf., vol. 26, no. January, pp. 180–192, 2019, doi: 10.1016/j.addma.2019.01.007.
11. S. R. Singh and P. Khanna, "Wire arc additive manufacturing (WAAM): A new process to shape engineering materials," Mater. Today Proc., vol. 44, pp. 118–128, 2021, doi: 10.1016/j.matpr.2020.08.030.
12. D. Ding, Z. Pan, D. Cuiuri, and H. Li, "Wire-feed additive manufacturing of metal components: technologies, developments and future interests," International Journal of Advanced Manufacturing Technology, vol. 81, no. 1–4. Springer London, pp. 465–481, Oct. 26, 2015. doi: 10.1007/s00170-015-7077-3.
13. B. Tomar, S. Shiva, and T. Nath, "A review on wire arc additive manufacturing: Processing parameters, defects, quality improvement and recent advances," Mater. Today Commun., vol. 31, no. January, p. 103739, 2022, doi: 10.1016/j.mtcomm.2022.103739.
14. S. K. Manjhi, P. Sekar, S. Bontha, and A. S. S. Balan, "Effect of CMT-WAAM Process Parameters on Bead Geometry, Microstructure and Mechanical Properties of AZ31 Mg Alloy," J. Mater. Eng. Perform., vol. 33, no. 16, pp. 8567–8581, 2024, doi: 10.1007/s11665-023-08498-w.
15. S. Li et al., "Comparative study on the microstructures and properties of wire+arc additively manufactured 5356 aluminium alloy with argon and nitrogen as the shielding gas," Addit. Manuf., vol. 34, Aug. 2020, doi: 10.1016/j.addma.2020.101206.
16. Köhler, M.; Hensel, J.; Dilger, K. Effects of Thermal Cycling on Wire and Arc Additive Manufacturing of Al-5356 Components. Metals 2020, 10, 952.
17. Fang, X.; Zhang, L.; Chen, G.; Dang, X.; Huang, K.; Wang, L.; Lu, B. Correlations between Microstructure Characteristics and Mechanical Properties in 5183 Aluminium Alloy Fabricated by Wire-Arc Additive Manufacturing with Different Arc Modes. Materials 2018, 11, 2075.